From a two-dimensional chemical pattern to a three-dimensional topology through selective inversion of a liquid–liquid bilayer

JULIEN LÉOPOLDÈS* AND PASCAL DAMMAN*

Laboratoire de Physicochimie des Polymères, Université de Mons Hainaut, 20, Place du Parc, Mons, B-7000, Belgium

*e-mail: julien.leopoldes@umh.ac.be; pascal.damman@umh.ac.be

Published online: 26 November 2006; doi:10.1038/nmat1787

Soft organic surfaces with more and more complex topologies are required daily to engineer appropriate microstructures for many different applications such as DNA array technology[1], biological optics for advanced photonic systems[2] and microfluidics[3,4]. Complementarily to conventional lithographic processes[5,6], several pioneering methods have been developed recently, by controlling phase separation of polymer blends[7,8], spinodal decomposition of homopolymers[9,10] or by using the action of additional external forces driving diverse instabilities[11,12]. Here we present a method that not only provides original concepts towards the three-dimensional (3D) structuring of liquids, on the basis of the synergistic effects of molecular diffusion and confined nucleation, but also suggests original solutions for the transport, mixing and filtering of small volumes of liquid. Through the intrinsic destabilization of a liquid–liquid bilayer, the 2D pattern of a chemically structured surface with 'hydrophilic' and 'hydrophobic' domains is transferred to a solid/liquid interface as a 3D topography with either 'positive' or 'negative' replication. This easy-to-use process has potential applications in various technological realms requiring a specific topography at interfaces such as microfluidics or biosensors.

For a broad range of applications from microfluidics to super-hydrophobic surfaces, an important technological issue is the control of the topology of surfaces at a micrometric scale. A highly popular system consists of an organic film adsorbed on a substrate and subsequent use of 'soft lithography' or self-structuring processes. On appropriate substrates, nanometric films are unstable and naturally tend to self-destruct by spinodal decomposition[9,13], therefore providing possibilities of patterning by controlling the wavelength of the instability[14]. Such films, prepared by spin coating, are however difficult to process on large surface areas. On the other hand, thicker micrometric films are very easy to deposit but are not subjected to such long-range van der Waals forces, hence their high stability. In the micrometric range, the surface processing is usually restricted to lithography or mechanical treatment.

To control the architecture of organic films, we suggest a self-driven process on the basis of the selective inversion of a liquid–liquid bilayer through diffusion and nucleation/growth. Diffusion of the liquid forming the upper layer (ethanol) through the liquid forming the bottom layer (polydimethylsiloxane, PDMS) is the trigger of the destabilization of the interface between PDMS and the substrate. Once ethanol molecules reach the substrate, droplets nucleate, resulting in a confined replacement of PDMS as a scheme predetermined by the spatial arrangement of 'hydrophilic' domains. This process results in the growth and coalescence of droplets leading to a three-dimensional (3D) structured PDMS layer. We show how chemical patterning of the substrate and film thickness drive and control the spatial extent of the destabilization, leading to well-controlled 3D architectures.

We used PDMS with a viscosity $\eta = 300\,\mathrm{Pa\,s}$. The substrate is a gold-coated silica wafer (referred to as Au), initially covered by a homogeneous self-assembled monolayer of hexadecanethiol (referred to as CH3), obtained from immersion in a 10^{-3} mol solution in ethanol for 24 h (ref. 15). This surface was patterned by a partial destruction of the monolayer with an ultraviolet lamp through a photomask according to either chessboard or parallel line patterns. This procedure results in alternating regions of Au/CH3. On Au and CH3 homogeneous surfaces, we measured the equilibrium contact angles θ^{PDMS} of PDMS droplets in ethanol, $\theta^{\mathrm{PDMS}}_{\mathrm{Au}} \sim 170^\circ$ and $\theta^{\mathrm{PDMS}}_{\mathrm{CH3}} = 30^\circ$. For ethanol droplets in PDMS, the contact angles $\theta^{\mathrm{ethanol}}$ are the supplementary ones, $\theta^{\mathrm{ethanol}}_{\mathrm{Au}} \sim 10^\circ$ and $\theta^{\mathrm{ethanol}}_{\mathrm{CH3}} = 150^\circ$. The surface tension between ethanol and PDMS is $\gamma = 1.6\,\mathrm{mN\,m^{-1}}$ (ref. 16) and the solubility of ethanol in PDMS is 5 ± 2 wt%.

Figure 1 shows the evolution of a 5-μm-thick PDMS film deposited on a Au/CH3 chessboard surface once immersed in ethanol. Surprisingly, such thick micrometric PDMS films (expected to be stable) undergo a rapid morphological transformation on all the Au patches simultaneously. The overall process only requires a few minutes to get a fully developed pattern (Fig. 1d), yet the apparition of smaller structures is observed within a few seconds (Fig. 1a–c). We emphasize that the thickness $h = 5\,\mu\mathrm{m}$ of the film used in this example ensures that the dispersive forces between the different interfaces are not relevant to our system, the films are thus not subjected to spinodal decomposition[9,17]. In fact, the destruction of the PDMS/Au interfaces occurs through diffusion of ethanol molecules and nucleation of ethanol droplets on all Au patches at the same time (Fig. 2).

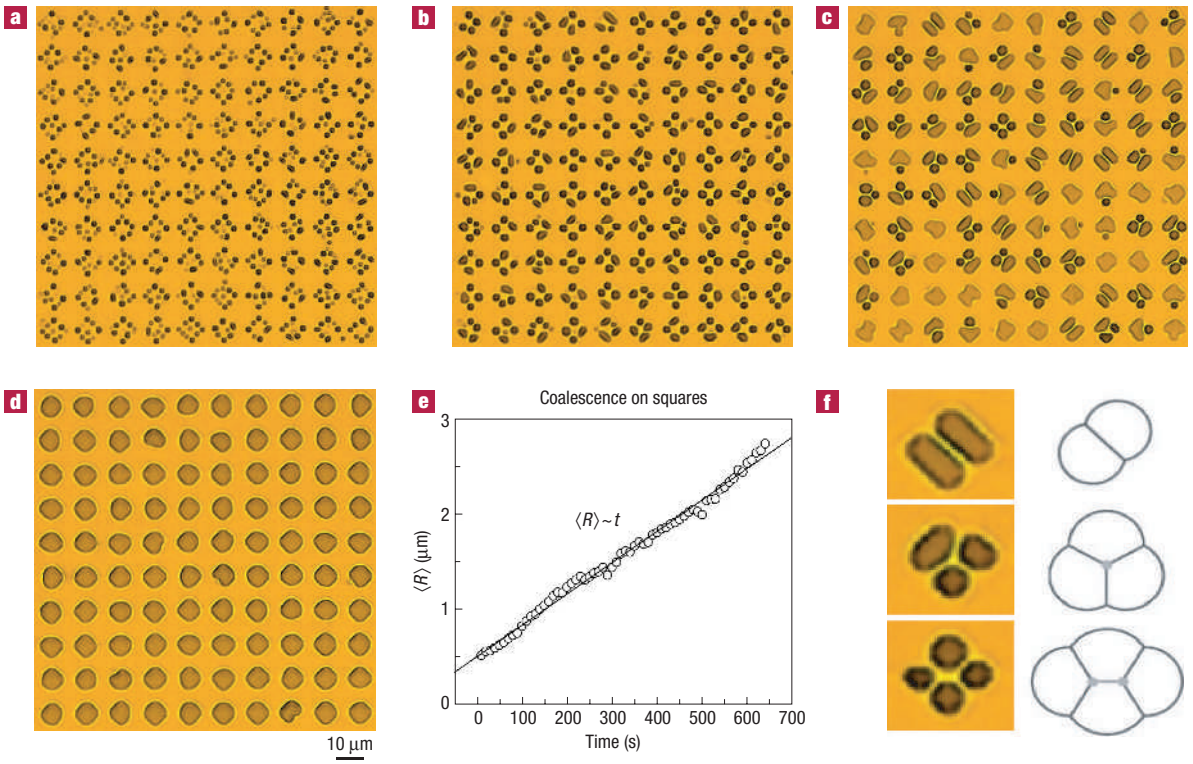

Figure 1 Optical micrographs of a PDMS film ($h_0 = 5.0\,\mu$m) deposited on a chemically patterned substrate and immersed in ethanol. We use a symmetric chessboard pattern with dimensions $a_{Au} = a_{CH3} = 8\,\mu$m. **a–d**, Images taken 1 min (**a**), 7 min (**b**), 13 min (**c**) and 20 min (**d**) after immersion. The darker regions correspond to the locations of Au patches, where ethanol droplets nucleate under PDMS (**a**). **b–d** show the growth and coalescence of ethanol droplets up to the final state where one droplet covers the whole of each Au part (**d**). During the process, the PDMS film on the CH3 squares (lighter areas) remains completely unaltered. **e**, Temporal evolution of the average droplet radius $\langle R \rangle$, following $\langle R \rangle \sim t$ (see text). **f**, Correlation between ethanol droplets separated by thin PDMS membranes and soap-bubble configurations.

Molecules are known to diffuse through a fluid according to a diffusion coefficient D given by the Stokes–Einstein relation $D = k_b T/6\pi\eta R$, where k_b is the Boltzmann constant, T is the temperature, η is the viscosity of the fluid and R is the radius of a sphere corresponding to the diameter of the diffusing particles[4]. Small molecules such as ethanol diffuse rapidly through the thin film, with a diffusion coefficient $D \sim 10^{-14}\,\mathrm{m^2\,s^{-1}}$ providing typical diffusion times close to 10 s for micrometric membranes.

The formation of an ethanol layer at the PDMS/substrate interface can be described by the excess intermolecular interaction free energy $\Delta G(h) = \Delta G^{LR}(h) + \Delta G^{SR}(h)$ with $\Delta G^{LR}(h)$ and $\Delta G^{SR}(h)$ corresponding to long- and short-range interactions respectively. The long-range component of the free energy is usually given by the relation $\Delta G^{LR} = -A/12\pi h^2$, where A is the Hamaker constant. The Hamaker constant can itself be computed from the dispersive component of the individual surface tensions, γ_i^D, by using the relation: $A_{132} = 24\pi\delta_0^2\,(\sqrt{\gamma_1^D} - \sqrt{\gamma_3^D})\,(\sqrt{\gamma_2^D} - \sqrt{\gamma_3^D})$, where δ_0 is an atomic cut-off distance, equal to 0.158 nm (ref. 18), corresponding to the interactions of two surfaces, 1 and 2, through a medium 3. The dispersive and polar components of the surface tensions for the various phases with air are for ethanol ($\gamma^D \sim 20$, $\gamma^P \sim 3\,\mathrm{mN\,m^{-1}}$), PDMS ($\gamma^D \sim 21$, $\gamma^P \sim 0\,\mathrm{mN\,m^{-1}}$), Au ($\gamma^D \sim 47$, $\gamma^P \sim 3\,\mathrm{mN\,m^{-1}}$) and CH3 ($\gamma^D \sim 22$, $\gamma^P \sim 0\,\mathrm{mN\,m^{-1}}$). Owing to the very low value of γ^D for ethanol, the Hamaker constant is positive for both surfaces ($A_{Au} \sim 10^{-21}\,\mathrm{J\,m^{-2}}$ and $A_{CH3} \sim 10^{-22}\,\mathrm{J\,m^{-2}}$) indicative of long-range attractive forces between both interfaces. For small thicknesses, the short-range forces dominate and $\Delta G(h \to 0) = S = \gamma(\cos\theta - 1)$ (ref. 17). Here, S is the spreading coefficient that represents the surface free-energy difference between dry and wet surfaces. As the spreading coefficient drastically changes by covering Au with alkanethiols ($S_{Au} \sim -0.02\,\mathrm{mN\,m^{-1}}$ and $S_{CH3} \sim -3\,\mathrm{mN\,m^{-1}}$), the excess free energy $\Delta G(h)$ must exhibit very different shapes. Such potentials are shown in Fig. 2e. For CH3, the 'dry' CH3 substrate is in equilibrium with macroscopic ethanol droplets in partial wetting. For Au, however, owing to the value of S close to 0, the 'dry' Au substrate is in equilibrium with an ultrathin film of ethanol, which is itself in equilibrium with macroscopic ethanol droplets. This situation (usually referred to as pseudo-partial wetting[17]) promotes the growth of macroscopic ethanol droplets because the activation energy describing the nucleation of ethanol droplets on an ethanol layer vanishes. On CH3 however, the nucleation must occur directly on the 'dry' surfaces with a very high nucleation barrier owing to the high contact angle ($\theta_{CH3}^{ethanol} = 150°$). This antagonistic situation explains why we observe a swift condensation of ethanol droplets solely on Au patches, whereas CH3 domains remain 'dry'.

The preferential formation of ethanol droplets at the boundaries between the two different patches (Fig. 1a) can be related to the diffusion process itself. The two-dimensional random walk of ethanol molecules at the PDMS/substrate interface, with a low mobility for high-energy Au patches and a higher mobility for low-energy CH3 patches, enhances the nucleation on the chemical boundaries, owing to a concentration gradient of diffusing molecules[19].

Despite the absence of a 'true' ethanol gas phase and the presence of a highly viscous PDMS layer, the mechanism involved in

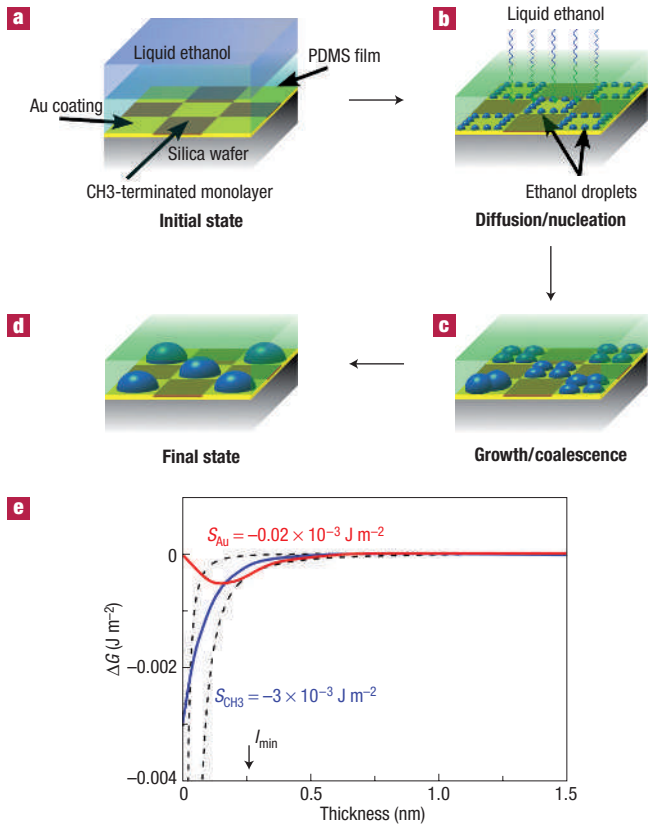

Figure 2 Sketch of the experimental set-up used for thin-film structuring. **a**, A PDMS film spin-coated on a microcontact printed gold-coated silica wafer and immersed in ethanol. **b**, After immersion, we observe diffusion of ethanol molecules through the PDMS film and nucleation of ethanol droplets intercalated between the PDMS film and the Au patches. **c**, Growth and coalescence of ethanol droplets confined to Au patches. **d**, The final morphology with single ethanol droplets located under PDMS on each Au square. **e**, Evolution of the intermolecular interaction free energy, ΔG, with the thickness, h, of an ethanol layer on Au (red) and CH3 (blue) surfaces in a PDMS environment (the spreading coefficients, S, are indicated). The dotted line represents the long-range component of ΔG computed from the relation $-A/12\pi h^2$ (A is equal to 10^{-21} J m^{-2} and 10^{-22} J m^{-2} for Au and CH3, respectively). The limit of short-range forces, l_{min}, is also indicated.

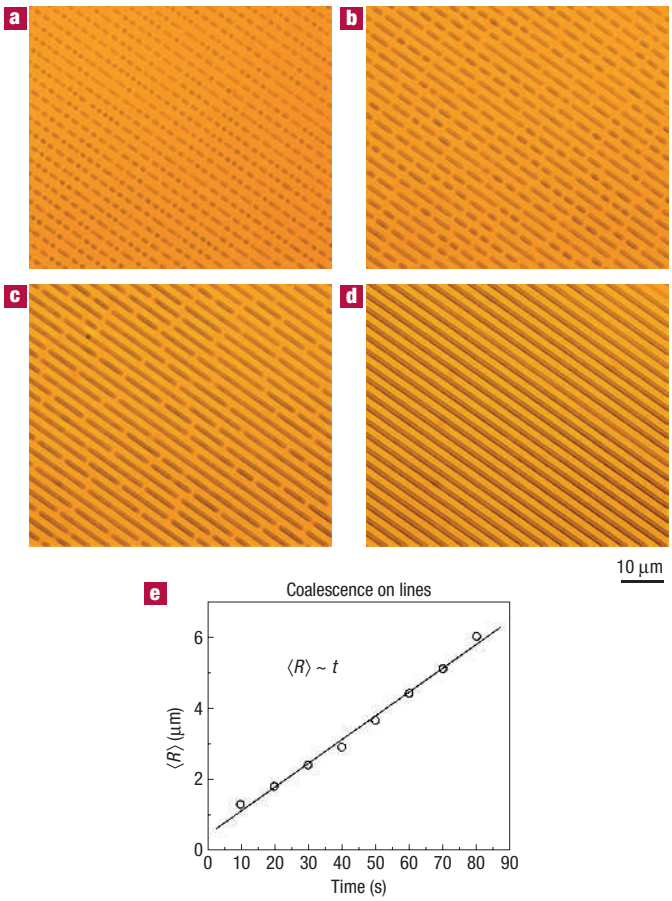

Figure 3 Optical micrographs of a PDMS film ($h_0 = 5.0$ μm) deposited on a substrate patterned by chemical stripes and immersed in ethanol. The pattern is symmetric with stripes of 2 μm wide. **a–d**, Images taken 1 min (**a**), 2 min (**b**), 3 min (**c**) and 4 min (**d**) after immersion. **e**, Temporal evolution of the average droplet radius $\langle R \rangle$, following $\langle R \rangle \sim t$ (see text).

the completion of the process (Fig. 2) is evocative of the formation of breath figures[19–24]. Its dynamics should be well described by general self-similar growth laws characterizing the evolution of the average drop radius $\langle R \rangle$ with time t (refs 22–24). For usual breath figures obtained from condensation of a gas phase on a solid substrate, $\langle R \rangle \sim t^{1/(D_d - D_s)}$. Here, D_d and D_s are the dimensionalities of the drop and of the substrate, respectively. We observed a linear increase of $\langle R \rangle$ with time for the chessboard patterns (Fig. 1e), consistent with $D_d = 3$ and $D_s = 2$ characterizing droplets on squares. This law remains valid as long as $\langle R \rangle$ remains smaller than the size of the chemical pattern, and is followed by a short transition regime to the final state. Interestingly, these observations confirm that chemical heterogeneities and surface topology have a similar role because this growth law is relevant to describe growth and coalescence of water droplets on a surface structured by grooves[24]. During the transition regime, the confined droplets self-organize with a spatial distribution following Plateau's rules for mechanical equilibrium (Fig. 1f). This phenomenon is due to the presence of a thin PDMS membrane separating each droplet, akin to the structure of 2D foams.

As shown in Fig. 3, this destabilization process has no restriction regarding the shape of the Au/PDMS interface. For chemical stripes, the structure of the initial pattern consists of droplets appearing as short dashes that grow and coalesce by the same mechanism as the one observed for the chessboard pattern, that is, via the bursting of the PDMS membranes. The final morphology is a set of hemispherical cylinders of ethanol liquid whose basis corresponds to the width of the chemical stripe. Identically to chessboard substrates, the kinetics of droplet growth follows a linear relationship $\langle R \rangle \sim t$ (Fig. 3e). This is consistent with the growth law, $\langle R \rangle \sim t^{1/(D_d - D_s)}$, by considering $D_d = 2$ and $D_s = 1$, adequately with two-dimensional droplets and one-dimensional substrate[24].

After full development of the process (Figs 1d and 3d), the long time morphology reflects a 'negative' replication of the chemically patterned surface. The topology of the PDMS film is selectively altered by the formation of ethanol droplets located on the Au patches. It should be noted that PDMS films on Au and CH3 are in partial wetting (that is, we observe non-zero contact angles) and may self-destruct via a dewetting process. For micrometric thicknesses however, the 3D sculpted films could remain in a

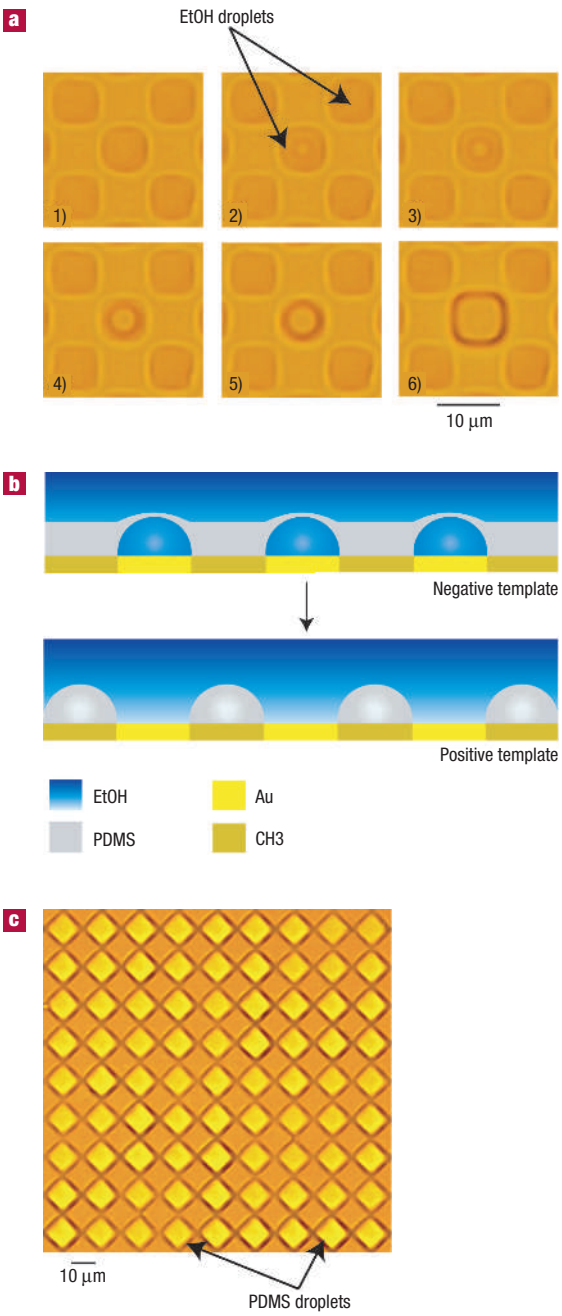

Figure 4 Details of the bursting process and resulting morphology. a, Optical micrographs recorded during the bursting of an ethanol droplet on an 8 μm chessboard-patterned surface after thinning of the PDMS film (initial thickness $h_0 = 0.6\,\mu m$). Successive images are recorded every 1/10 s (from left to right and top to bottom). **b**, Sketches of the morphologies corresponding to positive and negative replication of the chemical pattern. **c**, Optical micrograph of the final morphology obtained after completion of the bursting process for a PDMS film (initial thickness $h_0 = 0.6\,\mu m$) on a chessboard-patterned surface. The light regions correspond to PDMS droplets on CH3 patches (the darker regions correspond to pure ethanol).

metastable state for very long times because the dewetting must be artificially initiated by heterogeneous nucleation.

Then, a key point remains undefined at this stage: What is the equilibrium morphology of such liquid–liquid bilayers? As shown by Lipowsky and coworkers[25,26], the equilibrium morphology of a fluid on a chemically patterned surface is determined by the sum of all surface free-energy contributions and the volume V of the fluid normalized by the size (a) of the 'hydrophilic' patches, V/a^3. In the early stages, we observe the condensation of ethanol in a PDMS environment (Fig. 1a–d). For a symmetric chessboard pattern ($a_{Au} = a_{CH3}$), a collection of ethanol droplets on Au patches is expected as long as $V_{ethanol}/a^3 < 0.5$ (ref. 25). For thick PDMS layers ($h_0 > a/2$), the morphology of ethanol droplets under PDMS is therefore stable. As shown in Fig. 4, thin PDMS films ($h_0 < a/2$) behave differently and undergo a morphological transition that finally leads to a full reversal of the architecture of the system, generating small PDMS droplets on each CH3 patch in an ethanol environment (Fig. 4c). To evolve towards this inverted morphology, the PDMS film self-destructs by a bursting mechanism. The growth of ethanol droplets induces a thinning of the polymeric membrane above every Au patch. For thin PDMS films ($h_0 < a/2$), both PDMS/ethanol interfaces become rapidly separated by a distance at which attractive van der Waals interactions become significant ($h^* \sim 0.1\,\mu m$) (refs 18,27). As shown in Fig. 4a, this thinning process results finally in the local bursting of the film confined to the Au squares. We followed the opening of the holes by recording the bursting process with a camera operating at $10\,s^{-1}$ and found a maximum bursting velocity of $v \sim 20\,\mu m\,s^{-1}$. This value, more than two orders of magnitude higher than the typical dewetting velocity of PDMS on Au ($\sim 0.1\,\mu m\,s^{-1}$), is in agreement with the model proposed by Debregeas *et al.* for the viscous bursting of PDMS films[27]. In their model, the opening velocity reaches a maximum given by $v_{max} \sim 0.1L/\tau$, where τ and L are the relaxation time of the process given by $\tau = \eta h^*/\gamma$ and the dimension of the film, respectively. An estimate of τ by inserting our experimental parameters in the previous expression provides $\tau \sim 0.02\,s$, corresponding to $v_{max} \sim 30\,\mu m\,s^{-1}$ in accordance with the measured value. When the bursting process is complete, the initial morphology corresponding to ethanol droplets embedded by PDMS is fully reversed. This results in an alternative distribution of the two fluid phases, characterized by PDMS droplets in ethanol that form a very good 'positive' replication of the chemically patterned surface (Fig. 4b,c).

The method presented here is rapid, inexpensive and can be applied without limitations to various chemical patterns, provided to have a high contrast of wettability for 'hydrophilic' and 'hydrophobic' patches. As the diffusion of molecules and the controlled nucleation of liquid droplets are the main limiting steps governing the development of the selective inversion process, this concept provides a general method towards liquid structuring from macroscopic down to nanometric length scales. The dimensions and shape of the 3D structures can be easily tailored for specific applications by slight alteration of the surface free energies. Also, changing the thickness of the PDMS layer ($1\,\mu m < h_0 < 10\,\mu m$) leads to 3D patterns with either a positive or negative replication of the chemically patterned surface. After patterning, the PDMS films can be ultraviolet-cured and lifted off the substrate.

In addition to its ability to sculpt organic polymer surfaces, this new system is very promising in initiating novel microfluidic applications on the basis of the exchange, mixing, reaction or filtration of picolitre down to atolitre volumes of fluids, by controlling the diffusion coefficients and the selective nucleation of droplets on various chemically structured surfaces.

Received 14 June 2006; accepted 17 October 2006; published 26 November 2006.

References

1. Langer, R. & Tirrell, D. A. Designing materials for biology and medicine. *Nature* **428,** 487–492 (2004).
2. Lee, L. P. & Szema, R. Inspirations from biological, optics for advanced photonic systems. *Science* **310,** 1148–1150 (2005).

3. Delamarche, E., Juncker, D. & Schmid, H. Microfluidics for processing surfaces and miniaturizing biological assays. *Adv. Mater.* **17,** 2911–2933 (2005).
4. Squires, T. M. & Quake, S. R. Microfluidics: Fluid physics at the nanoliter scale. *Rev. Mod. Phys.* **77,** 977–1026 (2005).
5. Xia, Y., Rogers, J. A., Paul, K. E. & Whitesides, G. M. Unconventional methods for fabricating and patterning nanostructures. *Chem. Rev.* **99,** 1823–1848 (1999).
6. Xia, Y. *et al*. Complex optical surfaces formed by replica molding against elastomeric masters. *Science* **273,** 347–349 (1996).
7. Boltau, M., Walheim, S., Mlynek, J., Krausch, G. & Steiner, U. Surface-induced structure formation of polymer blends on patterned substrates. *Nature* **391,** 877–879 (1998).
8. Heriot, S. Y. & Jones, R. A. L. An interfacial instability in a transient wetting layer leads to lateral phase separation in thin spin-cast polymer-blend films. *Nature Mater.* **4,** 782–786 (2005).
9. Herminghaus, S. *et al*. Spinodal dewetting in liquid crystal and liquid metal films. *Science* **282,** 916–919 (1998).
10. Higgins, A. M. & Jones, R. A. L. Anisotropic spinodal dewetting as a route to self-assembly of patterned surfaces. *Nature* **404,** 476–478 (2000).
11. Schäffer, E., Thurn-Albrecht, T., Russell, T. P. & Steiner, U. Electrically induced structure formation and pattern transfer. *Nature* **403,** 874–877 (2000).
12. Schäffer, E., Harkema, S., Roerdink, M., Blossey, R. & Steiner, U. Morphological instability of a confined polymer film in a thermal gradient. *Macromolecules* **36,** 1645–1655 (2003).
13. Seemann, R., Herminghaus, S. & Jacobs, K. Dewetting patterns and molecular forces: A reconciliation. *Phys. Rev. Lett.* **86,** 5534–5537 (2001).
14. Kargupta, K. & Sharma, A. Templating of thin films induced by dewetting on patterned surfaces. *Phys. Rev. Lett.* **86,** 4536–4539 (2001).
15. Love, J. C., Estroff, L. A., Kriebel, J. K., Nuzzo, R. G. & Whitesides, G. M. Self-assembled monolayers of thiolates on metals as a form of nanotechnology. *Chem. Rev.* **105,** 1103–1169 (2005).
16. Bico, J. & Quéré, D. Self-propelling slugs. *J. Fluid Mech.* **467,** 101–127 (2002).
17. de Gennes, P.-G., Brochard-Wyart, F. & Quéré, D. *Capillarity and Wetting Phenomena: Drops, Bubbles, Pearls, Waves* (Springer, New-York, 2004).
18. Reiter, G. *et al*. Thin film instability induced by long-range forces. *Langmuir* **15,** 2551–2558 (1999).
19. Schäffle, C., Leiderer, P. & Bechinger, C. Subpattern formation during condensation processes on structured substrates. *Europhys. Lett.* **63,** 394–400 (2003).
20. Lopez, G. P., Biebuyck, H. A., Frisbie, C. D. & Whitesides, G. M. Imaging of features on surfaces by condensation figures. *Science* **260,** 647–649 (1993).
21. Kumar, A. & Whitesides, G. M. Pattern condensation figures as optical diffraction gratings. *Science* **263,** 60–62 (1994).
22. Steyer, A., Guenoun, P. & Beysens, D. Growth of droplets on a substrate by diffusion and coalescence. *Phys. Rev. A* **44,** 8271–8277 (1991).
23. Viovy, J. L., Beysens, D. & Knobler, C. M. Scaling description for the growth of condensation patterns on surfaces. *Phys. Rev. A* **37,** 4965–4970 (1988).
24. Narhe, R. D. & Beysens, D. A. Nucleation and growth on a superhydrophobic grooved surface. *Phys. Rev. Lett.* **93,** 076103 (2004).
25. Lenz, P. & Lipowsky, R. Morphological transitions of wetting layers on structured surfaces. *Phys. Rev. Lett.* **80,** 1920–1923 (1998).
26. Gau, H., Herminghaus, S., Lenz, P. & Lipowsky, R. Liquid morphologies on structured surfaces: From microchannels to microchips. *Science* **283,** 46–49 (1999).
27. Debregeas, G., de Gennes, P.-G. & Brochard-Wyart, F. The life and death of "bare" viscous bubbles. *Science* **279,** 1704–1707 (1998).

Acknowledgements

We wish to thank D. Beysens, S. Dietrich, A. Jonas and G. Reiter for fruitful discussions. This work was supported by the Belgian National Funds for Scientific Research (FNRS), the Government of the Region of Wallonia (CORRONET Research Programme) and the European Commission (Phasing out, MateriaNova). P.D. is a research Associate of the FNRS.

Correspondence and requests for materials should be addressed to J.L. or P.D.

Competing financial interests

The authors declare that they have no competing financial interests.